Microenvironment in the Corona Region of Triblock Copolymer Micelles: Temperature Dependent Solvation and Rotational Relaxation Dynamics of Coumarin Dyes

Manoj Kumbhakar,* Teena Goel, Sukhendu Nath, Tulsi Mukherjee, and Haridas Pal*

Radiation & Photochemistry Division, Bhabha Atomic Research Center, Mumbai 400 085, India

Received: June 20, 2006; In Final Form: October 6, 2006

Dynamic Stokes' shift and fluorescence anisotropy measurements using coumarin-153 (C153) and coumarin-151 (C151) as the fluorescence probes have been carried out in aqueous poly(ethylene oxide)$_{20}$-poly(propylene oxide)$_{70}$-poly(ethylene oxide)$_{20}$ (P123) and poly(ethylene oxide)$_{100}$-poly(propylene oxide)$_{70}$-poly(ethylene oxide)$_{100}$ (F127) block copolymer micelles with an aim to understand the water structures and dynamics in the micellar corona region. It has been established that the probes reside in the micellar corona region. It is indicated that the corona regions of P123 and F127 micelles are relatively less hydrated than the Palisade layers of neutral micelles like Triton-X-100 and Brij-35. From the appraisal of total Stokes' shift values for the probes in the two block copolymer micelles, it is inferred that the F127 micelle is more hydrated than the P123 micelle. It is observed that the dynamic Stokes' shift values for both of the probes remain more or less similar at all the temperatures studied in the P123 micelle. For C153 in F127, however, the observed Stokes' shift is seen to decrease quite sharply with temperature, though it remains quite similar for C151. Moreover, the fraction of the unobserved initial dynamic Stokes' shift is appreciably higher for both the probes in the F127 micelle compared to that in P123. Over the studied temperature range of 293−313 K, the spectral shift correlation function is described adequately by a bi-exponential function. Rotational relaxation times for C153 in both the micelles show a kind of transition at around 303 K. These results have been rationalized assuming collapse of the poly(ethylene oxide) (PEO) blocks and formation of water clusters in the corona region due to dehydration of poly(ethylene oxide) blocks with an increase in temperature. A dissimilar probe location has been inferred for the differences in the results with C153 and C151 probes in F127. Comparison of the microviscosity and the hydration of the block copolymer micelles has also been made with those of the other commonly used neutral micelles, for a better understanding of the results in the block copolymer micelles.

1. Introduction

Water-soluble triblock copolymers of poly(ethylene oxide) (PEO) and poly(propylene oxide) (PPO) are denoted as PEO-PPO-PEO. Variations in the PPO/PEO ratio of the copolymers allow one to tune their properties to meet specific requirements in different applications. Formation of micelles is a direct consequence of the anisotropic interaction between water and copolymer blocks in certain temperature ranges.[1,2] The PEO blocks are soluble in water over a wide range of temperatures, from 273 to 373 K, while the PPO blocks dissolves only below ∼288 K.[3,4] As a result, in dilute aqueous solutions, copolymers exist as monomers at lower temperatures. However, with an increase in temperature and/or concentration, copolymer chains tend to aggregate to form spherical micelles. Thus, above a specific temperature (critical micellization temperature, CMT) or concentration (critical micellization concentration, CMC), triblock copolymers undergo micelle formation, where the PPO blocks form the hydrophobic core and the PEO blocks form the hydrophilic shell (or corona) of the micelles.[1−12] These amphiphilic copolymers consisting of both reasonably hydrophilic (PEO) and reasonably hydrophobic (PPO) blocks are an important class of surfactants having extensive applications in the areas of controlled drug delivery and release, dispersion technology, nanomaterial synthesis, etc.[14−20] In pursuit of these micellar systems as new models for confined reaction media, thorough understanding of the micellar characteristics is a prerequisite. Various chemical reactions such as electron transfer, charge transfer, etc. that occur in organized media and in biological systems are largely controlled by the microenvironment around the reactants.[21−28] Hence, prior knowledge of the microenvironment around the reactants is very important in controlling various processes in confined media. There has been a concise effort in exploring the structure and various other properties of block copolymer micelles by employing techniques like NMR, static and dynamic light scattering, neutron scattering, fluorescence techniques, etc.[29−40] Efforts have also been made in the understanding of the interactions of the probe molecules with the micellar internal environments and their dynamics.[7,35−41]

Studies on solvation and rotational relaxation dynamics in organized assemblies are very useful in exploring the microenvironments around the probe molecules.[7,26−28,35−40,42−46] In the present work, we have investigated the solvation dynamics and the fluorescence anisotropy decay dynamics in aqueous PEO_{20}-PPO_{70}-PEO_{20} (P123) and PEO_{100}-PPO_{70}-PEO_{100} (F127) solutions above the CMT, using coumarin-153 (C153) and coumarin-151 (C151) as the fluorescence probes. The CMT values of the copolymers are concentration dependent. In the present study, we have used 5% weight/volume (W/V) aqueous solutions of P123 and F127, where block copolymer micelles are formed above 285.5 and 292.5 K, respectively (CMT).[5] Various micellar properties of 5% W/V P123 and F127 are reported in the literature, and some of these properties are listed

* Corresponding authors. E-mail: manojk@magnum.barc.gov.in (M.K.). E-mail: hpal@apsara.barc.gov.in (H.P.). Fax: 91-22-25505151/25519613.

10.1021/jp063839v CCC: $33.50
Published on Web 12/08/2006

TABLE 1: List of the Important Parameters of P123 and F127 Micelles (5% W/V Aqueous Solution) at Different Temperatures[a]

temp (K)	CMC[b] (% W/V)	N_{agg}[b]	r_c[b] (nm)	r_h[b] (nm)	τ_m (ns)	τ_0 (ns) C153	τ_0 (ns) C151
			P123				
293	0.18					5.99	6.12
298	0.03	86	5.20	5.77	174.2	6.05	6.09
303	0.005	211	7.10	7.96	402.9	5.93	6.03
308	0.001	244	7.30	8.18	388.1	5.87	5.98
313		287	7.70	8.63	407.0	5.79	5.95
			F127				
298	0.7	37	3.90	5.70	167.9	5.17	5.87
303	0.1	67	4.70	6.94	303.1	5.17	5.85
308	0.25	82	5.10	7.40	367.5	5.09	5.77
313	0.008	97	5.40	7.85	438.7	5.04	5.77

[a] The fluorescence lifetimes (τ_0) of C153 and C151 dyes in P123 and F127 micelles and the rotational relaxation times (τ_m) of the whole micelles of P123 and F127 at different temperatures are also listed. [b] The different micellar parameters are abbreviated as follows: CMC = critical micellization concentration; N_{agg} = micellar aggregation number; r_c = micellar core radius; r_h = hydrodynamic radius of the micelle. The values of different micellar parameters are taken from refs 2, 5, 6, and 35.

in Table 1 as a function of temperature.[2,5,6,35] There are some recent reports that aim to understand the details of the microenvironments in block copolymer micelles and membranes using fluorescence spectroscopic techniques.[35−41] Grant et al.[7,36] and Dutt[35] have shown that due to the micellization of block copolymers above the CMT, different probes experience significantly higher microviscosity in aqueous PEO_{109}-PPO_{41}-PEO_{109} (F88) and P123 solutions. The absence of a sharp change in microviscosity during micelle to gel transition has also been reported by Grant et al.[36] Humpolichova et al. have recently reported solvation dynamics in polystyrene-polyvinylpyridine-polyoxyethylene micelles.[39] The excitation wavelength dependence of solvation dynamics in the P123 micelle has also been reported by Sen et al. using coumarin-480 (C480) as the probe.[40] In spite of all these studies, the influence of temperature on the hydration characteristics of triblock copolymers micelles is not understood clearly. The aim of the present study is to comprehend the effect of temperature on the dynamics of the water molecules in the micellar corona region and that on the microviscosity experienced by the probes in the two triblock copolymer micelles. Besides knowing the effect of PEO chain lengths in P123 and F127 micelles on the probe microenvironments, our aim has also been to compare the present solvation and rotational relaxation dynamics results with our earlier works in other normal micelles like Triton-X-100 (TX-100) and Brij-35 (BJ-35).[26] Interestingly, in TX-100 and BJ-35 micelles, it was indicated that both micellar size and hydration play significant roles in determining the solvent relaxation dynamics for a probe in the micellar Palisade layer. As reported in the literature, unlike the TX-100 micelle, the micellar hydrodynamic radius of P123 and F127 does not change significantly with temperature.[2,5,6] Thus, a comparison of the present results in P123 and F127 micelles with those in normal micelles like TX-100 and BJ-35 is expected to give more insight into the effect of micellar size and hydration on the solvation dynamics in micellar media. Chemical structures of C153 and C151 probes are shown in Chart 1.

CHART 1

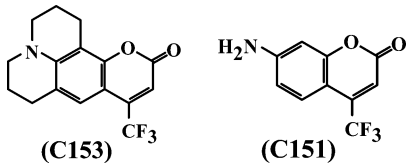

2. Experimental Details

The P123 and F127 copolymers were obtained from Aldrich and Sigma, respectively, and used without further purification. Laser grade C153 and C151 dyes were obtained from Exciton, USA, and used as received. The organic solvents used in the present work were of spectroscopic grade and obtained either from Spectrochem (India), SISCO Research Laboratories (India), S.D. Fine Chemical (India), or E. Merck (India). The nanopure water, having a conductivity of ~0.1 μS cm^{-1}, was obtained by passing distilled water through a Barnstead nanopure water system and used for the preparation of the aqueous micellar solutions.

In the experimental solutions, the concentration of P123 and F127 was kept at 5% W/V. The required amount of the block copolymers was taken by weighing and was kept overnight under refrigeration after adding the requisite amount of water in sealed containers. Samples for measurements were prepared by adding C153 and C151 dyes in the aqueous solutions of the block copolymers at room temperature. A rough estimation of the micelle concentrations ([M]) in the solution were evaluated from the concentration ([S]) of the block copolymers, the CMC of the copolymer micelles, and the average aggregation number (N_{agg}) of these micelles, using a simple relation like [M] = ([S] − CMC)/N_{agg}.[23,24] The micelle concentrations thus used are typically of the order of 10^{-4} M. In comparison to these micelle concentrations, the concentrations of the C153 or C151 dyes used were much lower, only in the range of 1−5 μM. With this experimental condition, the possibility of more than one probe occupying a single micelle can be ignored. Such a situation is important to avoid the effect of any dye−dye interaction on the observed solvation and rotational relaxation dynamics results.

Steady-state absorption spectra were recorded using a Jasco (Tokyo, Japan) model V530 spectrophotometer. Fluorescence spectra were recorded using a Hitachi (Tokyo, Japan) model F-4010 spectrofluorimeter. Time-resolved fluorescence measurements were carried out using a diode-laser-based, time-correlated single-photon-counting (TCSPC)[47] spectrometer from IBH, UK. In the present work, a 408 nm diode laser (1 MHz) was used as the excitation source and a TBX4 detection module (IBH, UK) coupled with a special Hamamatsu PMT was used for the fluorescence decay measurements. For the present setup, the instrument response function was ~230 ps at the full width at half-maximum (fwhm). The time resolution achievable with the present setup following deconvolution analysis of the fluorescence decays is about 50 ps.[47] For solvation dynamics studies, fluorescence decays were recorded at the magic angle (54.7°) with respect to the vertically polarized excitation light. Measurements were repeated three times, both to check the reproducibility and to obtain the average values of the relaxation times. In the present work, the temperature of the solution was varied with the help of a coldfinger arrangement and the temperature was controlled within ±1 °C using a microprocessor-based temperature controller (model DS from IBH).

Time-resolved emission spectra (TRES) were generated from a set of fluorescence decays collected at different wavelengths, covering the entire emission band of the probe. All the decays were fitted as three exponential functions. The emission spectrum at a given time t, $S(\lambda,t)$, was obtained from the series of the fitted decays, $D(\lambda,t)$, after their normalization with respect

TABLE 2: List of the Absorption (λ_{abs}^{max}) and Fluorescence (λ_{flu}^{max}) Maxima of C153 and C151 Dyes in Various Solvents and in Different Micelles at Ambient Temperature

		λ_{abs}^{max} (nm)		λ_{flu}^{max} (nm)	
medium	ϵ	C153	C151	C153	C151
cyclohaxane	2.02	393	348	455	410
decanol		418	378	517	476
octanol	8.1	420	380	520	478
hexanol	13.3	421	382	522	479
butanol	17.5	422	384	525	480
P123		420	381	515	475
F127		423	381	530	489
TX-100		427	382	536	490
TX-165		428	382	539	491
BJ-35		429	383	536	491

to the steady-state fluorescence spectrum, $S_0(\lambda)$, and using the following equation,[48]

$$S(\lambda,t) = D(\lambda,t)\frac{S_0(\lambda)}{\int_0^\infty D(\lambda,t)\,dt} \quad (1)$$

The method used to obtain the spectral shift correlation function $C(t)$ from the time-resolved emission spectra is similar to that described by Maroncelli and Fleming.[48] In the construction of the $C(t)$ curve, the steady-state fluorescence spectrum $S_0(\lambda)$ was used as the infinite time spectra. Such a consideration is justified because the solvation times in the present systems are faster than the fluorescence lifetimes of the probes used (cf. section 3.C).

Fluorescence anisotropy studies were carried out by measuring the polarized fluorescence decays, $I_{II}(t)$ and $I_{\perp}(t)$, where $I_{II}(t)$ and $I_{\perp}(t)$ are the fluorescence decays for parallel and perpendicular polarizations with respect to vertically polarized excitation light. From $I_{II}(t)$ and $I_{\perp}(t)$ decays, the anisotropy decay function $r(t)$ was constructed using the following relation,[47]

$$r(t) = \frac{I_{II}(t) - GI_{\perp}(t)}{I_{II}(t) + 2GI_{\perp}(t)} \quad (2)$$

where G is a correction factor for the polarization bias of the detection setup. The G factor was independently determined by using the horizontally polarized excitation light and measuring the two perpendicularly polarized fluorescence decays with respect to the excitation polarization.

3. Results and Discussions

3.A. Steady-State Measurements. In P123 and F127 micellar solutions, the solubility of both C153 and C151 probes is seen to increase substantially, though the solubility of these dyes in water is very low.[45,46] It is thus indicated that in the present cases the C153 and C151 dyes are preferentially solubilized in P123 and F127 micelles. Considering that the present dyes are reasonably polar in nature (due to their intramolecular charge transfer (ICT) character)[23−27] and that the solubilities of these dyes are quite high in polar protic solvents, like methanol, ethanol, hexanol, etc., it is expected that these dyes in P123 and F127 micelles preferentially reside in the micellar corona region of intermediate polarity. To obtain an additional support for this, steady-state absorption and fluorescence spectra of both the dyes in various alcoholic solvents have been measured at room temperature along with those in different neutral micelles, namely, Triton-X 100 (TX-100), Triton-X 165 (TX-165), Brij-35 (BJ-35), P123, and F127. The absorption and fluorescence

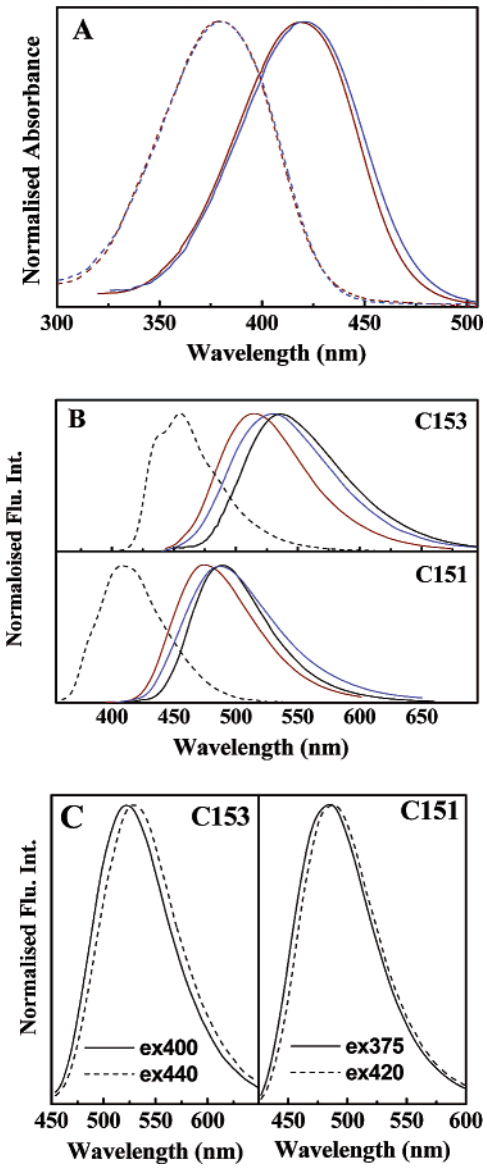

Figure 1. (A) Absorbance spectra of C153 (solid line) and C151 (dashed line) in P123 (red) and F127 (blue) micellar solution. (B) Fluorescence spectra of C153 (top) and C151 (bottom) in cyclohexane (black dashed line), P123 micelles (red solid line), F127 micelles (blue solid line), and TX-100 micellar (black solid line) media. (C) Emission spectra of C153 and C151 in F127 micellar solution at different excitation wavelengths.

maxima thus obtained are listed in Table 2. A comparison of the absorption spectra of the C153 and C151 dyes, as shown in Figure 1A , reveals that the micropolarity for C151 is quite similar in both P123 and F127 micelles, although C153 shows slightly higher micropolarity in the F127 micelle compared to that in the P123 micelle. In the case of Triton-X micelles (e.g., TX-100 and TX-165), it has been observed that, with an increase in the oxoethylene chains, the degree of hydration of the micelle increases.[46] Due to a prevailing similar situation in the present case, we can expect more hydration in the F127 micelle in comparison to that in P123. Therefore, a small red shift in the absorption spectra of C153 dye in the F127 micelle compared to that in the P123 micelle is possible. The fact that the probes, C153 and C151, show somewhat different features in relation to the micropolarity in P123 versus F127 micelles is probably due to the differences in the solubilization sites of the probes in the micelles. The dyes C153 and C151 are expected to be somewhat different in their hydrophobicity. The amino hydro-

gens of probe C151 can participate in the hydrogen bond formation with the solvent molecules, which is not possible for the former dye. Thus, C151 can show some hydrophilic character and thus will prefer to reside more toward the micellar surface in comparison to the site of locations of the C153 dye in the micelles. From the consideration of the hydrodynamic radius (r_h) and core radius (r_c) of the micelles (cf. Table 1), the corona thicknesses of P123 and F127 micelles are estimated to be in the range of about 6−10 Å for the former and about 20−25 Å for the latter micelles at different temperatures. The effective diameter of C151 and C153 probes are estimated to be about 7.8 and 6.8 Å, respectively, as estimated following Edward's volume addition method.[49] For the P123 micelle, since the corona thickness is comparable to the probe dimension, the solubilization sites are expected to be quite similar for both C151 and C153 probes in the P123 micelle. For the F127 micelle, however, the solubilization sites of C151 and C153 probes can vary significantly because the corona thickness is larger than the probe dimension and the hydrophobicities of the two probes are reasonably different. It is thus likely that, in the F127 micelle, the C153 dye resides somewhat deeper in the corona region while the C151 dye resides reasonably closer to the micellar surface. Accordingly, it is possible that dye C151 recognizes a nearly similar environment in both P123 and F127 micelles but C153 recognizes a somewhat different environment in the two micelles.

Figure 1B shows the steady-state fluorescence spectra of C153 and C151 dyes in both the micelles at room temperature along with those in the TX-100 micelle, for a comparison. As expected, the fluorescence spectrum of C153 in F127 is ∼15 nm red shifted compared to that in P123, due to the increased hydration of the former micelle. A similar red shift is also observed for the C151 dye in F127 in comparison to that in P123, though the absorption spectra of the dye do not show any significant difference in the two micelles. This could be due to the following two reasons. It is possible that the steady-state emission spectra of the dye measured in the P123 micelle do not correspond to the fully relaxed spectra. Such a situation can arise if the solvent relaxation dynamics is slower than the decay rate of the excited state of the probe. As will be discussed latter in section 3.C, the fluorescence lifetimes of the dyes are about two times higher than even the slower component of the solvation times. Under this situation, it is expected that the steady-state emission spectra will effectively be similar to the fully relaxed spectra. The other possible reason for the additional red shift in the fluorescence spectra of the C151 dye in the F127 micelle could be the solute−solvent intermolecular hydrogen bonding interaction.[50−56] It has been observed that the fluorescence spectra of the coumarin dyes undergo an extra red shift of about 10−15 nm due to intermolecular hydrogen bonding with protic solvents.[55,56] With a reasonably lesser number of water molecules in the micellar phase, the effect of the intermolecular hydrogen bonding interaction may not be that substantial in the P123 micelle in comparison to that in the more hydrated F127 micelle. Hence, an additional red shift in the emission spectra of the C151 dye in F127 in comparison to that in the P123 micelle is expected. Since absorption spectra are less sensitive to the polarity changes and the solute−solvent hydrogen bonding interactions, no significant shift is observed in the absorption spectra of the C153 dye in the F127 micelle in comparison to that in P123. In this context, the work of Lee et al.[41] is worth mentioning. It has been shown by these authors that in block copolymer membranes the red shift in the fluorescence spectra of a polarity sensitive probe of ICT character is directly related to the extent of the water penetration in the membrane. Since the coumarin dyes are also of ICT character and their fluorescence spectra are quite sensitive to the solvent polarity, a similar situation can also be expected with respect to the water penetration in the block copolymer micelles. Thus, drawing an analogy with the results of Lee et al., we can infer that the larger red shifts in the fluorescence spectra of the probes C153 and C151 in the F127 micelle in comparison to that in the P123 micelle is due to the higher hydration of the former micelle than the later.

In normal micelles, like TX-100, TX-165, and BJ-35, the polarity (defined in terms of dielectric constant, ϵ) of the microenvironment around the probe C153 is reported to be ∼27.[24] Considering the polarity of the corona region of P123 and F127 micelles to be around that of hexanol/butanol (envisaged from the comparison of absorption and fluorescence maxima of the probes; cf. Table 2), corresponding ϵ values in the two micelles are expected to be within the range of ∼10−15.[57] Thus, the corona region of P123 and F127 micelles is indicated to be much less hydrated than the Palisade layer of the neutral micelles like TX-100, TX-165, and BJ-35.

It has been found that the emission maxima of both C151 and C153 probes in P123 and F127 micelles are marginally dependent on the excitation wavelength, although the fwhm remains almost similar. Figure 1C shows the emission spectra of C153 and C151 at different excitation wavelengths in the F127 micelle. The observed red edge excitation shift is ∼10 and ∼5 nm for C153 (excitations at 400 and 440 nm) and C151 (excitations at 375 and 420 nm), respectively. These results indicate a somewhat broader distribution of the probes in the block copolymer micelles. A similar excitation wavelength-dependent shift of about 25 nm in the emission maxima of coumarin-480 (C480) dye has also been reported in 1% P123 micellar solution by Sen et al.[40] With the present probes, the shift is much less compared to that reported by Sen et al. for C480 dye. Steady-state fluorescence spectra of both C151 and C153 probes in P123 and F127 micelles were recorded in the temperature range of 293−313 K, with 5 deg temperature intervals. Almost similar fluorescence spectra were obtained in both the micelles at different temperatures studied, indicating no significant change in polarity for the probe microenvironment.[41]

3.B. Time-Resolved Anisotropy Measurements. The fluorescence decays of C151 and C153 dyes in P123 and F127 micelles were measured at the emission maxima of the dyes as a function of temperature. These decays were recorded at the magic angle (54.7°) with respect to the vertically polarized excitation light. The decays are seen to fit well with a single-exponential function. It is observed that the fluorescence lifetimes (τ_0, listed in Table 1) of the dyes do not change significantly with temperature. These results suggest that the microenvironments of the two micelles do not change significantly for the temperature range studied. These results are thus in accordance with the steady-state results discussed in section 3.A.

In the present work, fluorescence anisotropy decays of the two probes in P123 and F127 micelles were measured as a function of temperature, following the procedure given in section 2. Anisotropy decays in the present systems are seen to follow a bi-exponential nature, a behavior reported in the literature for many other micellar systems.[26,27,35,42−44] Fluorescence anisotropy decays of C151 in P123 micellar solutions at 293 and 313 K are shown in Figure 2A. Rotational relaxation times for the present systems along with their relative contributions at

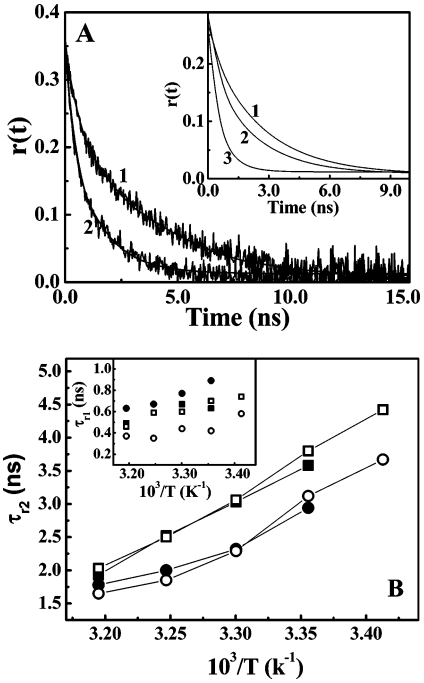

Figure 2. (A) Fluorescence anisotropy decays of C151 in P123 micellar solutions at 293 K (1) and 313 K (2). The solid line represents the bi-exponential fitted curves. (inset) Fluorescence anisotropy decays (only fitted curves are shown) of C153 in P123 (1), TX-100 (2), and BJ-35 (3) micellar solutions at 298 K. (B) Plot of the τ_{r2} and τ_{r1} (inset) values as a function of the inverse of temperature for C153 in P123 (−○−), C151 in P123 (−□−), C153 in F127 (−●−), and C151 in F127 (−■−) micellar solutions.

different temperatures are listed in Table 3. The average rotational relaxation times ($<\tau_r>$), as calculated for the present systems using the following relation, are also listed in Table 3.

$$<\tau_r> = a_{r1}\tau_{r1} + a_{r2}\tau_{r2} \quad (3)$$

where τ_{r1} and τ_{r2} are the fast and the slow time constants and a_{r1} and a_{r2} are their relative contributions, respectively.

As well being discussed in the literature,[26,27,35,42−44] the fluorescence anisotropy decay of a probe in a micelle is determined by the interplay of three different motions. They are (i) the wobbling motion of the probe in the micelle, which occurs with a time constant of τ_w, (ii) the lateral diffusion of the probe along the curved micellar surface, which occurs with a time constant of τ_l, and (iii) the rotation of the whole micelle, which occurs with a time constant of τ_m. As treated in the well-known two-step model,[43,44] due to the interplay of the above three motions, the anisotropy decay of a probe in a micelle effectively follows a bi-exponential function, where the two rotational time constants, τ_{r1} and τ_{r2}, are related to the time constants τ_w, τ_l, and τ_m by the following relations.

$$\tau_{r1}^{-1} = \tau_w^{-1} + \tau_{r2}^{-1} \quad (4)$$

$$\tau_{r2}^{-1} = \tau_l^{-1} + \tau_m^{-1} \quad (5)$$

For both the micelles, the τ_m values can approximately be estimated using the Stokes−Einstein−Debye equation as[26,27,35,42−44]

$$\tau_m = \frac{4\pi r_h^3 \eta}{3k_B T} \quad (6)$$

TABLE 3: List of the Time Constants and Their Relative Contributions as Obtained from the Bi-exponential Analysis of the Fluorescence Anisotropy Decays of C153 and C151 Dyes in 5% Aqueous Solutions of P123 and F127 as a Function of Temperature[a]

probe	T (K)	r_0	τ_{r1} (ns)	a_{r1} (%)	τ_{r2} (ns)	a_{r2} (%)	$<\tau_r>$ (ns)	S
				P123				
C153	293	0.35	0.58 ± 0.1	9.48	3.67 ± 0.1	90.52	3.38	0.95
	298	0.35	0.42 ± 0.1	8.46	3.12 ± 0.1	91.54	2.89	0.96
	303	0.33	0.44 ± 0.1	9.39	2.29 ± 0.1	90.61	2.12	0.95
	308	0.31	0.35 ± 0.1	13.60	1.85 ± 0.1	86.40	1.65	0.93
	313	0.30	0.37 ± 0.1	23.66	1.65 ± 0.1	76.34	1.35	0.87
C151	293	0.36	0.74 ± 0.1	6.69	4.42 ± 0.1	93.31	4.17	0.97
	298	0.35	0.70 ± 0.1	8.35	3.80 ± 0.1	91.65	3.54	0.96
	303	0.34	0.60 ± 0.1	12.60	3.06 ± 0.1	87.40	2.75	0.93
	308	0.32	0.59 ± 0.1	15.77	2.50 ± 0.1	84.23	2.20	0.92
	313	0.31	0.46 ± 0.1	15.72	2.03 ± 0.1	84.28	1.78	0.92
				F127				
C153	298	0.32	0.89 ± 0.1	21.9	2.94 ± 0.1	78.1	2.49	0.88
	303	0.31	0.77 ± 0.1	20.8	2.32 ± 0.1	79.8	2.01	0.89
	308	0.31	0.67 ± 0.1	26.3	2.00 ± 0.1	73.7	1.65	0.86
	313	0.30	0.63 ± 0.1	32.8	1.78 ± 0.1	67.2	1.40	0.82
C151	298	0.34	0.63 ± 0.1	13.6	3.58 ± 0.1	86.4	3.18	0.93
	303	0.32	0.67 ± 0.1	19.6	3.03 ± 0.1	80.4	2.57	0.90
	308	0.31	0.59 ± 0.1	17.0	2.52 ± 0.1	83.0	2.19	0.91
	313	0.30	0.49 ± 0.1	24.5	1.93 ± 0.1	75.5	1.58	0.87

[a] The average rotational relaxation times ($<\tau_r>$), the initial anisotropy values (r_0), and the values of the structural parameter *S* are also listed for all the cases.

where η is the viscosity of water and r_h is the hydrodynamic radius of the micelle. Table 1 lists the τ_m values of the two micelles estimated at different temperatures. It is seen that the τ_m values are always more than one order of magnitude higher than even the longer τ_{r2} values obtained from the experimental anisotropy decays. Thus, we can assume that the contribution of the whole micelle rotation to the observed anisotropy decays is negligible. Accordingly, from eq 5, the experimental τ_{r2} value effectively measures the time constant τ_l for the lateral diffusion of the probe in the micelle. Similarly, τ_{r2} being about 5−8 times higher than the τ_{r1} values, we can expect from eq 4 that the τ_{r1} value effectively measures the time constant τ_w for the wobbling motion of the probe in the micelle.

In the two-step model, a generalized structural parameter *S* is also defined to express the anisotropy decays in their normalized form (normalized to the initial anisotropy r_0) as[43,44]

$$r(t) = (1 - S^2)\exp(-t/\tau_{r1}) + S^2 \exp(-t/\tau_{r2}) \quad (7)$$

Thus, the parameter *S* is related to the experimentally determined a_{r2} value as

$$S = \sqrt{a_{r2}} \quad (8)$$

The *S* values estimated for C153 and C151 probes in P123 and F127 micelles at different temperatures are listed in Table 3. In the micellar core, as the polymer chains do not have any orderliness, the microenvironment in the core should be more like a homogeneous nonpolar liquid. Thus, if the probe resides in the micellar core, its wobbling motion is expected to be almost isotropic, resulting the *S* value being close to zero and the fluorescence anisotropy decay being effectively single-exponential.[26,35,42−44] The substantially higher *S* values as estimated in the present cases thus suggest that the probes do not reside in the micellar core but preferentially reside in the micellar corona region where the surfactant chains are expected to be arranged in a much more orderly manner.[26,35,40,42−44] In

block copolymer micelles, though the hydration mainly occurs in the corona region constituted by the PEO blocks, the core region constituted by the PPO blocks can also contain few water molecules.[2,5,6] Thus, the core of these micelles will not be as dry as that of the normal micelles. Therefore, in block copolymer micelles, the location of probe C153 may extend beyond the corona region toward the core. In fact, reports of Grant et al.[7,36] on the microenvironment of the probes investigated by fluorescence spectroscopy have suggested that C153 resides in the core of the F88 block copolymer micelle. In spite of several efforts, the exact location of C153 in block copolymer micelles is yet to be described properly. Probe dissolved in the micellar core is expected to show single-exponential fluorescence anisotropy decay.[26,35,42−44] As discussed in the earlier part of this section and also from the reports of Grant et al., it is seen that the rotational decay dynamics of C153 is bi-exponential in nature. It is thus difficult to conceive that the dye C153 solubilized in the core of the present micelles. Moreover, the largest change in the microviscosity due to micellization is expected to occur in the most orderly arranged head group (corona) region of the micelle.[26,27,35,40,42−46] Hence, present results as well as those of Grant et al.[7,36] perhaps indicate that the main solubilization site of the C153 dye is the corona region of the block copolymer micelles.

A detailed analysis of the anisotropy decays following a two-step model is a very involved process.[43,44] However, from the experimentally determined τ_{r1} and τ_{r2} values, we can obtain some qualitative idea about the changes in the microviscosity of the corona region of the block copolymer micelles. Changes in τ_{r2} values with temperature, as shown in Figure 2B, indicate a gradual decrease in the microviscosity around the probe on increasing the temperature. The decrease in the rotational relaxation times with temperature is possibly due to the inverse relation of viscosity with temperature.[57,58] Thus, even though the hydration of the block copolymer micelle reduces with temperature,[2,5,6,35] the microviscosity experienced by the probe in the micelle shows a decreasing trend with temperature. Although the τ_{r1} values are relatively more fluctuating, a decrease in the τ_{r1} values with temperature is quite evident from the present results (cf. Figure 2B inset). Higher fluctuations in the τ_{r1} values are, probably, related to the limitation in the recovery of these values due to finite time resolution of our TCSPC setup.

A close look into the temperature-dependent changes in the τ_{r2} values (cf. Figure 2B) indicate that, for the C153 dye in both P123 and F127 micelles, apparently there are two different slopes: one above and one below about 303 K. The slope above ~303 K seems to be significantly lower than that below ~303 K. The somewhat lower slope above ~303 K possibly indicates that, over and above the temperature effect on viscosity, there could also be an additional effect for the higher microviscosity at elevated temperatures. We presume that at higher temperatures the PEO chains undergo a kind of collapse due to their large dehydration. Due to this dehydration and also due to an increase in the aggregation number at elevated temperatures,[2,5,6,35] the PEO chains come closer to each other, resulting a larger resistance to the rotational dynamic of the probe.[27] Although dehydration of PEO blocks is expected to occur monotonously above the CMT, the extent of dehydration is possibly much higher above ~303 K, resulting in the collapse of the PEO chains in the micellar corona region. Interesting to note that the influence of the micellar dehydration at higher temperatures is not that clearly reflected in the anisotropy results with C151 dye. This is possibly due to the fact that the dehydration of the block copolymer micelles initiates from the interior of the corona region. Thus, dye C151 residing near the micellar surface does not experience the changes as effectively as probe C153 residing deep inside the micellar corona region.

Recently, an extensive study on the rotational relaxation dynamics of some hydrophobic probes in 1% W/V aqueous P123 solution has been reported by Dutt.[35] Comparing the present results with those of Dutt, it is seen that the rotational relaxation dynamics in the present cases with coumarin dyes in 5% W/V aqueous P123 solution are qualitatively very similar to those observed by Dutt for other hydrophobic probes. A similar decreasing trend in the rotational relaxation times with the increase in the temperature has also been reported by Grant et al. in F88 micellar solution.[36] Comparing the rotational relaxation times for C151 and C153 probes, it is indicated from Table 3 that the rotational relaxation is somewhat slower for the former probe than the latter in both the micelles. This we attribute to the preferred H-bonding interaction of C151 dye with the available water molecules around the probe in the micellar corona region, causing the rotational relaxation dynamics of the dye to be slower.

At this juncture, it is worth comparing the microviscosity in the corona region of P123 and F127 micelles with those of the Palisade layer of other neutral micelles. Fluorescence anisotropy decays of the C153 dye in P123, TX-100, and BJ-35 micelles at 298 K are shown in the inset of Figure 2A. It is evident from this figure that the microviscosity experienced by the probe in the P123 micelle is higher than that in TX-100 and BJ-35 micelles (roughly 2 and 4 times that of TX-100 and BJ-35 micelles, respectively).[26] These results are in accordance with the fact that the P123 micelle is much less hydrated than TX-100 and BJ-35 micelles, as discussed in section 3.A. The microviscosity experienced by the probe in F127 is in between that of P123 and TX-100. The higher microviscosity in P123 is perhaps also due to the higher aggregation number of the micelle in comparison to that of the F127 micelle (cf. Table 1).

3.C. Time-Resolved Fluorescence Measurements. Wavelength-dependent changes in the fluorescence decays obtained for both C153 and C151 dyes in P123 and F127 micellar solutions indicate the presence of time-dependent Stokes' shifts for the emission spectra at all the temperatures studied.[26−28] Typical such fluorescence decays of C153 in P123 at 308 K are shown in Figure 3A. The time-resolved emission spectra (TRES) of the probes in the two micelles at different temperatures were generated using the spectral reconstruction method described in the literature.[48] Typical TRES for C153 in P123 micellar solution at 308 K are shown in Figure 3B. The dynamic Stokes' shifts $\nu(t)$ of the TRES were used to construct the normalized correlation function $C(t)$ as[48]

$$C(t) = \frac{\nu(t) - \nu(\infty)}{\nu(0) - \nu(\infty)} \tag{9}$$

where $\nu(0)$, $\nu(t)$, and $\nu(\infty)$ correspond to the frequencies of the emission maxima at times 0, t, and ∞, respectively.

The $C(t)$ curves as obtained for C153 and C151 dyes in P123 and F127 micellar solutions at different temperatures are shown in Figure 4. It should be noted that, due to faster solvation, a significant fraction of the initial dynamic Stokes' shift is beyond the time resolution of our present measurement. Thus, only the slower part is observed in the present experiments. This is clearly indicated by the comparison of the $\Delta\bar{\nu}^{sol}_{obs}$ and $\Delta\bar{\nu}^{sol}_{total}$ values, the observed and total expected Stokes' shifts due to the solvation process (cf. Table 4). For the present systems, the $\Delta\bar{\nu}^{sol}_{total}$

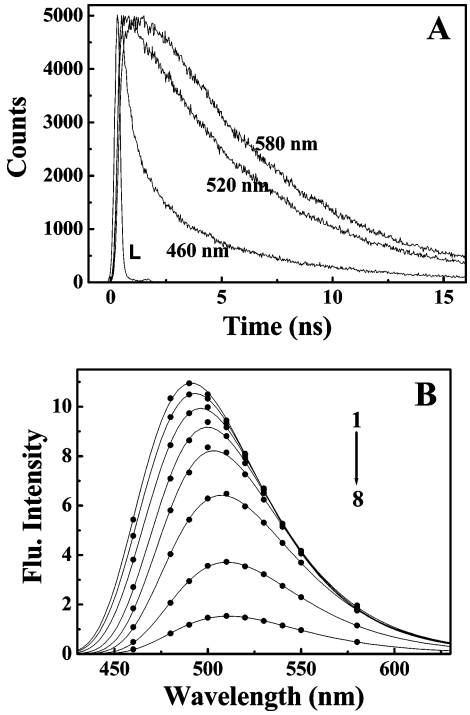

Figure 3. (A) Typical fluorescence decays obtained at different wavelengths for the C153 dye in 5% P123 micellar solution at 308 K. The decays at the blue edge of the steady-state fluorescence spectra show a distinct fast decay component, and those at the red edge of the steady-state fluorescence spectra show a distinct growth component, indicating a time-dependent Stokes' shift in the emission spectra of the dye in micellar solution. (B) Time-resolved emission spectra of C153 in 5% P123 micellar solution at 308 K. For spectra 1−8, the time windows are 0.05, 0.10, 0.20, 0.40, 0.80, 2.00, 5.00, and 10.00 ns, respectively. The symbols in the spectra correspond to the experimental points, and the continuous curves correspond to the log-normal fits to the experimental data points.

values were estimated from the Stokes' shifts for the probes in a nonpolar solvent cyclohexane and in the block copolymer micelle, as obtained from the absorption and the steady-state fluorescence spectra. It is seen that the $\Delta\bar{\nu}_{obs}^{sol}$ values are always much lower than the $\Delta\bar{\nu}_{total}^{sol}$ values. It is expected that the contribution of the fast solvation component will increase with an increase in temperature. As a larger part of the dynamic Stokes' shift corresponding to the fast solvation component is missed in the present measurements, the temperature effect on the observed $C(t)$ curves mainly shows the changes on the slower part of the solvation process. For the P123 micelle, the temperature effect on the observed $C(t)$ curves is not very evident (cf. Figure 4A and B). In the F127 micelle, however, the $C(t)$ curves show a sharp change at the temperatures between 303 and 308 K (cf. Figure 4C and D), suggesting a distinct change in the micellar corona region at these temperatures.

It is clearly indicated from the $C(t)$ curves that the solvation dynamics in both P123 and F127 micelles follow a non-single-exponential behavior. Solvation time constants for the present systems were obtained following a bi-exponential analysis of the $C(t)$ curves.[26−28] The values of the solvation times (τ_{s1} and τ_{s2}) along with their respective percentage contributions (a_{s1} and a_{s2}) are listed in Table 4. In the present context, it is important to mention that the solvation times estimated for the present systems are much shorter than the fluorescence lifetimes of the probes (τ_0 values in Table 1). Thus, the use of the steady-state fluorescence spectra of the probes as the infinite time fluorescence spectra, as required for the construction of the $C(t)$ curves, is quite justified for the present systems.

It is expected that the changes in the $C(t)$ curves with temperature will reflect the temperature-dependent changes in the hydration characteristics of the micelles. As mentioned earlier, due to limited time resolution of our TCSPC setup (∼50 ps; cf. section 2), we always missed a significant amount of the initial dynamic Stokes' shifts corresponding to the fast solvation component. We expect that this fast solvation component arises due to the combined effect of the inertial motion of the entrapped water molecules in the micelle and the segmental motion of the PEO chains of the surfactant molecules. The dynamic Stokes' shifts we observe in the present study are mainly due to the slow orientation of the water molecules around the probe that occurs in hundreds of picoseconds to nanoseconds. In the construction of the $C(t)$ curves, in the present work, we always used the initial spectra obtained at the shortest possible time window (∼50 ps, following the deconvolution analysis of the fluorescence decays) with the present TCSPC setup. The total dynamic Stokes' ($\Delta\bar{\nu}_{total}^{sol}$) shifts for C153 and C151 dyes in the P123 micelle were expected to be around 925 and 849 cm^{-1}, respectively. In the present study, observed dynamics Stokes' shifts ($\Delta\bar{\nu}_{obs}^{sol}$) are around 800 and 600 cm^{-1} for C153 and C151 dyes, respectively, in the P123 micelle. Thus, the initial about 15−30% of the dynamic Stokes' shifts associated with the fast solvation component could not be observed in the present measurements. Almost similar results were obtained for C153 and C151 dyes in the P123 micelle at all the temperatures studied, indicating a comparable microenvironment for the probes at all the temperatures, as also inferred earlier in section 3.A. Similarly, the total Stokes' shift expected in F127 is 1306 cm^{-1} for C153 and 1433 cm^{-1} for C151, which are much higher than the values expected in the P123 micelle. A higher degree of hydration in F127 owing to the larger PEO chain length compared to that of P123 leads to the higher Stokes' shifts in the former micelle. The interesting observation from the dynamic Stokes' shift is that the observed shift ($\Delta\bar{\nu}_{obs}^{sol}$) for the C153 dye in the F127 micelle decreases quite drastically with temperature. At low temperature, 298 K, there is not much of the fast solvation component. With an increase in temperature, the contribution of the fast solvation component increases and as a result less than about 60% of the total dynamics Stokes' shift ($\Delta\bar{\nu}_{total}^{sol}$) is actually observed at 313 K. On the contrary, a large Stokes' shift is missing for the C151 dye in the F127 micelle, even at lower temperatures. In this case, the percentage missing of the Stokes' shift only marginally increases with temperature. Therefore, it is evident that the microenvironments for C153 and C151 dyes are not similar in the F127 micelle.

Figure 5 shows the changes in the $\Delta\bar{\nu}_{obs}^{sol}$ values for the present systems with temperature. It is interesting to note from Figure 5 that the $\Delta\bar{\nu}_{obs}^{sol}$ values for the C153 dye in the F127 micelle show a sudden dip for the temperatures above about 303 K. For the C151 dye in the F127 micelle, though the effect is not very prominent, there is a significant decrease in the $\Delta\bar{\nu}_{obs}^{sol}$ value at 313 K. In the P123 micelle, no such effect is, however, indicated with either of the probes used. Present results indicate that in the F127 micelle the microenvironment certainly undergoes a sudden change above about 303 K, possibly due to enhanced dehydration of the micelle at elevated temperatures. Comparing the results with those of C151 and C153 dyes in the F127 micelle, it is also indicated that the dehydration of the micelle possibly starts from the interior of the corona region, as also inferred earlier from the fluorescence anisotropy results.

Following literature reports, the PEO blocks of the copolymer micelles undergo substantial dehydration with temperature. Thus, the solvation dynamics was expected to become slower on

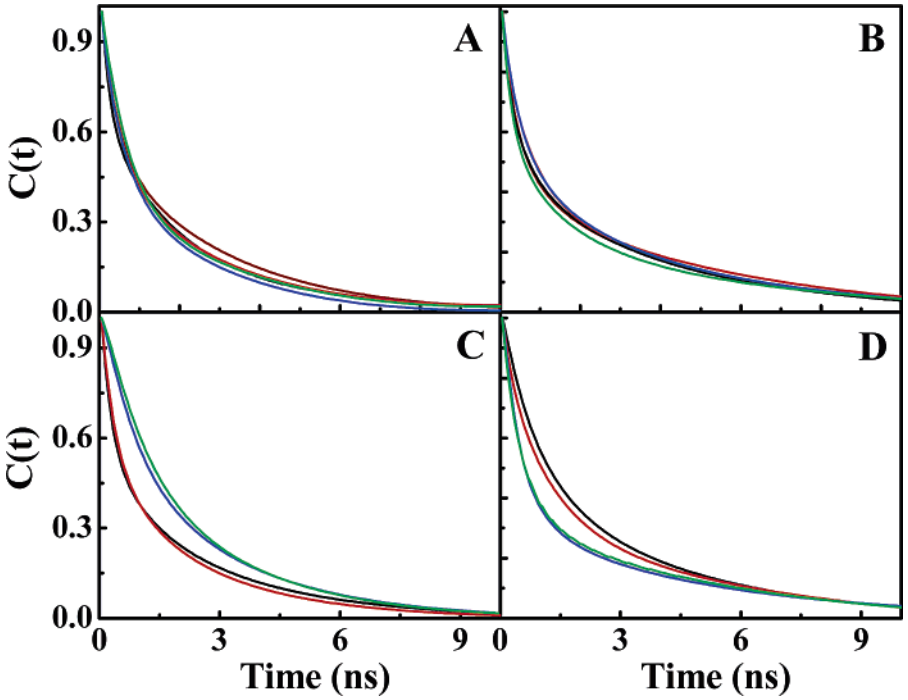

Figure 4. Normalized spectral shift correlation functions $C(t)$ at 293 (brown line), 298 (black line), 303 (red line), 308 (blue line), and 313 K (green line) for C153 in P123 (A), C151 in P123 (B), C153 in F127 (C), and C151 in F127 (D) micellar solutions.

TABLE 4: Solvation Times and Their Relative Contributions as Obtained from the Bi-exponential Analysis of the Normalized Spectral Shift Response Function $C(t)$ for C153 and C151 Dyes in P123 and F127 Micellar Solution at Different Temperatures above the CMT[a]

						$\Delta\bar{\nu}^{sol}$ (cm^{-1})	
probe	T (K)	τ_{s1} (ns)	a_{s1} (%)	τ_{s2} (ns)	a_{s2} (%)	$\Delta\bar{\nu}^{sol}_{obs}$	$\Delta\bar{\nu}^{sol}_{total}$
				P123			
C153	293	0.35 ± 0.1	44.4	2.60 ± 0.1	55.6	834	925
	298	0.22 ± 0.2	45.8	2.23 ± 0.1	54.2	870	
	303	0.38 ± 0.1	48.3	2.42 ± 0.1	51.7	735	
	308	0.46 ± 0.1	51.2	2.48 ± 0.1	48.8	787	
	313	0.56 ± 0.1	54.4	2.55 ± 0.1	45.6	700	
C151	293	0.37 ± 0.1	54.5	3.65 ± 0.1	45.5	648	849
	298	0.33 ± 0.1	50.5	3.32 ± 0.1	49.5	680	
	303	0.50 ± 0.1	55.0	3.57 ± 0.1	45.0	630	
	308	0.47 ± 0.1	52.0	3.59 ± 0.1	48.0	580	
	313	0.31 ± 0.2	55.3	3.26 ± 0.1	44.7	600	
				F127			
C153	298	0.30 ± 0.1	53.2	2.62 ± 0.1	46.8	1282	1306
	303	0.36 ± 0.1	52.1	2.40 ± 0.1	47.9	1183	
	308	0.99 ± 0.1	54.1	3.63 ± 0.1	45.9	836	
	313	1.31 ± 0.1	64.7	4.22 ± 0.1	35.3	767	
C151	298	0.84 ± 0.1	51.2	4.06 ± 0.1	48.8	511	1452
	303	0.68 ± 0.1	52.0	3.80 ± 0.1	48.0	522	
	308	0.46 ± 0.1	68.0	4.23 ± 0.1	32.0	500	
	313	0.46 ± 0.1	64.9	4.69 ± 0.1	35.1	403	

[a]The observed ($\Delta\bar{\nu}^{sol}_{obs}$) and the expected ($\Delta\bar{\nu}^{sol}_{total}$) dynamic Stokes' shift values for the present systems are also listed.

increasing the temperature. Accordingly, the difference between $\Delta\bar{\nu}^{sol}_{total}$ and $\Delta\bar{\nu}^{sol}_{obs}$ was expected to reduce with temperature. Observed Stokes' shift values for C153 in F127 (larger difference between $\Delta\bar{\nu}^{sol}_{total}$ and $\Delta\bar{\nu}^{sol}_{obs}$), however, depict an opposite picture than that expected. The results suggest a faster solvation at elevated temperatures causing $\Delta\bar{\nu}^{sol}_{obs}$ to drop significantly. As suggested earlier, the missing Stokes' shift in the present measurements must be due to a fast solvation component and it could be related to either the segmental motion of the PEO chains[40] or the inertial motion of the entrapped water

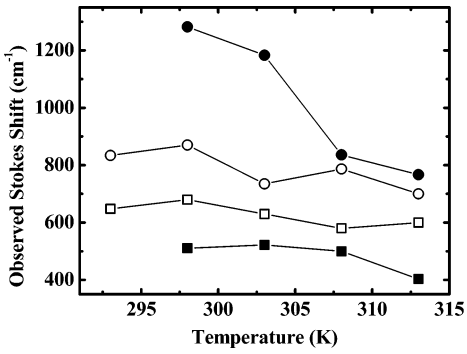

Figure 5. Observed stokes shift due to solvation ($\Delta\bar{\nu}^{sol}_{obs}$) as a function of temperature for C153 in P123 (−○−), C151 in P123 (−□−), C153 in F127 (−●−), and C151 in F127 (−■−) micellar solutions.

molecules in the micellar corona region.[60−62] In a recent study on the solvation dynamics of C480 dye in 1% P123 micelle solution with a time resolution of ∼350 fs, a time constant of about 60 ps has been observed by Sen et al.[40] and assigned to the segmental motion of the surfactant chains. This is in accordance with the molecular dynamics simulation results on polyethers by Olander et al.[59] From excitation-dependent solvation results, it has been inferred by Sen et al. that the micellar core as well as its periphery displays similar segmental motions. Thus, the probe locations apparently do not alter the fast solvation component to any great extent. Moreover, the contribution of this fast solvation component is observed to be relatively small, only ∼14%. In relation to the present results, the enhancement in the segmental motion of the surfactant chains with temperature cannot solely account for the large decrease in the $\Delta\bar{\nu}^{sol}_{obs}$ values for the C153 dye in the F127 micelle. This is so because the enhancement in the segmental motion and the consequent increase in the fast solvation component with temperature is expected to be quite gradual and fairly similar for all the probe−micelle combinations. In the present study with limited time resolution, though we cannot comment on the time scale of the fast solvation, the results certainly indicate that it is not only the segmental motions of

the surfactant chains but something else that is also responsible for the enhancement in the fast solvation component for the C153 dye in the F127 micelle.

The PEO-PPO-PEO block copolymer micelles can broadly be compared with the Triton-X series of micelles, especially with respect to the behavior of the water molecules present in the micellar phase. This we expect because the same oxoethylene chains are involved in the formation of the corona region of the block copolymer micelles and the Palisade layer of the Triton-X series of micelles. As expected, the water molecules in the micelle can exist either in the hydrogen bonded forms with the oxoethylene groups (thermodynamically bound) or just as the mechanically trapped water.[26,27,60] As the micelle undergoes dehydration (either by increasing the temperature or adding electrolytes in the solution), the bound water content in the micelle decreases with a concomitant increase in the mechanically trapped water.[26,27,60] In the TX-100 micelle, various groups have reported that as the oxoethylene groups undergo dehydration due to an increase in the temperature or in the presence of added electrolytes, the mechanically trapped water molecules form some clusters inside the micelle.[60−62] As the corona region of the block copolymer micelles resembles the Palisade layer of the TX-100 micelle, we can expect a similar kind of water cluster formation in the corona region at elevated temperatures, though the extent of such cluster formation may vary significantly depending on the degree of hydration of the micelle concerned. We thus propose that the formation of such water clusters is the main origin of the enhanced component of the fast solvation for the C153 dye in the F127 micelle at temperatures above 303 K, leading to a large decrease in the $\Delta\bar{\nu}_{obs}^{sol}$ values. The absence of such a sharp decrease in the $\Delta\bar{\nu}_{obs}^{sol}$ values in the P123 micelle with an increase in the temperature is possibly due to the lower hydration of the micelle that does not favor water cluster formation. As already inferred earlier, the degree of hydration is as such lower for the block copolymer micelles in comparison to that in the Triton-X micelles. Hence, the extent of water cluster formation will in general be less in block copolymer micelles than in the TX-100 micelle.

It is expected that with an increase in the temperature there will be an enhancement in the exchange rate between the mechanically trapped and the thermodynamically bound (H-bound to oxoethylene chains) water molecules in the micelle. Though the exchange of the bound and mechanically trapped water molecules in the micelle is mainly responsible for the slow nanosecond solvation component, as suggested by Nandi et al.,[63] it can also have some influence on the fast solvation component. It is thus possible that the interplay of all the above factors including the changes in the micellar size, hydration, and relative location of the probes ultimately determines the actual solvation dynamics, which is apparently temperature independent in the P123 micelle but significantly dependent in the F127 micelle. For the present cases, however, it is not possible to separate out the individual contributions of the different factors and thus to correlate them with the observed temperature effect on the solvation dynamics and the missing dynamic Stokes' shifts.

At this point, it is worth comparing the results of τ_{r2}, $\Delta\bar{\nu}_{obs}^{sol}$, and $C(t)$ as a function of temperature for both the probes in P123 and F127 micelles. It is evident that above 303 K the microviscosity increases more than expected (cf. Figure 2B), the spectral shift correlation function $C(t)$ shows sudden change (cf. Figure 4C and D), and $\Delta\bar{\nu}_{obs}^{sol}$ values reduce quite sharply (cf. Figure 5 for the C153 dye) in the F127 micelle. These changes in the F127 micelle seem to be related to the enhanced dehydration of the PEO blocks at temperatures above about 303 K. At these temperatures, collapse of the PEO blocks due to dehydration increase the microviscosity in the corona region. Simultaneously, the mechanically trapped water content increases at the expense of the thermodynamically bound water molecules, resulting in the formation of some water clusters in the micellar corona region. As the response of these water molecules is comparatively faster than the bound water molecules, it leads to a faster solvation dynamics.[27,45] As a result of the PEO chain collapse and the water cluster formation around 308 K in the F127 micelle, we thus observe a sharp change in the solvation and in the rotational relaxation dynamics in the F127 micelle. Results in the P123 micelle do not show any such behavior in the temperature range studied, perhaps due to the lower hydration of this micelle in comparison to that of the F127 micelle.

In comparing the solvation times for C151 and C153 probes in the two micelles, it is indicated that the τ_{s2} component is somewhat longer for the former probe than the latter. This is possibly due to the hydrogen bonding interaction of C151 dye with the available water molecules surrounding it in the micelle, which is expected to have a retarding effect on the reorientation dynamics of the water molecules adjacent to the probe and consequently a longer τ_{s2} component.

In our earlier studies in normal micelles like TX-100, BJ-35, and TX-165, it was indicated that the solvation rate decreases with a decrease in the micellar hydration.[26,39] Thus, due to greater hydration, solvation times in the BJ-35 micelle were observed to be 3−4 times shorter than those in the TX-100 micelle.[26] Therefore, from the consideration that the corona region of the P123 micelle is less hydrated ($\epsilon \sim 13$) than the Palisade layer of the TX-100 micelle ($\epsilon \sim 27$), a slower solvation rate was expected in the former micelle than in the latter. Interestingly, however, it is observed that the solvation times in the P123 micelle are almost in a similar range to those in the TX-100 micelle. Such an observation indicates that not only the micellar hydration but also some other factor also play a significant role in determining the solvation dynamics in the P123 micelle. We feel that the later factor is associated with the micellar size or more specifically the thickness of the micellar corona region. Unlike in the TX-100 micelle, where the Palisade layer is very thick ($\delta_r \sim 25$ Å),[24] the corona region of the P123 micelle is quite thin ($\delta_r \sim 6-9$ Å). Thus, the solvation dynamics in the P123 micelle is expected to be largely influenced by the water molecules just outside the micellar surface.[26] As the response of these water molecules is much faster than those inside the micelle, the former will largely subdue the effect of the reduced hydration of the P123 micelle on the observed solvation dynamics. It should be mentioned here that the mobility of the water molecules present just outside the micellar surface is not as fast as that of those in the bulk water. Although it is clear from the Stokes' shift measurements that the solvation is quite fast in the F127 micelle compared to that in the P123 micelle for both of the probes, it will be erroneous to compare the solvation times in the former micelle with those in the later, because the extent of the dynamics Stokes' shifts that are missing in the present measurements is quite different for different micelles at different temperatures.

4. Conclusions

Steady-state absorption and fluorescence studies of C153 and C151 dyes in 5% W/V aqueous solutions of P123 and F127 block copolymer above the CMT indicate that the probes

solubilize mainly in the micellar corona region. Both steady-state and time-resolved results indicate that the degree of hydration is greater in the F127 micelle in comparison to that in the P123 micelle. A significant part of the initial dynamic Stokes' shifts is seen to be missing in the present measurements due limited time resolution of our TCSPC setup. This missing fraction of the Stokes' shift is attributed to a fast solvation component arising due to the combined effect of the inertial motion of entrapped water molecules in the micelle and the segmental motion of the PEO chains of the surfactant molecules. Interconversion of thermodynamically bound and mechanically trapped water molecules is attributed to give rise to the slow nanosecond solvation component in the present systems. Fluorescence anisotropy results indicate a somewhat higher microviscosity at temperatures above 303 K for C153 in both the micelles. This is attributed to the collapse of PEO blocks due to their higher dehydration at elevated temperatures. The dehydration of the block copolymer micelles possibly initiates from the interior of corona region, as indicated by the differences in the fluorescence anisotropy and solvation dynamics results with C153 and C151 probes in the two micelles. Faster solvation for the C153 dye in the F127 micelle above 303 K, as indicated by a sudden drop in the observed dynamic Stokes' shift values, is attributed to the formation of water clusters in the micellar corona region as a consequence of the enhanced dehydration of the PEO blocks at elevated temperatures. The effect of this water cluster formation is, however, seen not to be that significant for probe C151, as the dye solubilizes near the micellar surface. Almost unaltered solvation for the C153 dye in P123 is possibly due to the lower hydration of this micelle in comparison to that of the F127 micelle. In brief, present results indicate that the water structures and the dynamics in the corona region of the block copolymer micelle are significantly dependent on the composition of the PPO and PEO blocks as well as on the relative locations of probes in the micellar phase.

References and Notes

(1) Alexandridis, P.; Lindman, B. *Amphiphilic Block Copolymers: Self-assembley and applications*; Elsevier: New York, 2000.

(2) Chu, B.; Zhou, Z. Physical chemistry of polyoxyalkylene block copolymer surfactants. In *Nonionic Surfactants*; Nace, V. M., Ed.; Surfactant Science Series; Marcel Dekker: New York, 1996; Vol. 60, p 67.

(3) Yang, J.; Wegner, G. *Macromolecules* **1992**, *25*, 1786.

(4) Mortensen, K.; Pedersen, J. S. *Macromolecules* **1993**, *26*, 805.

(5) Alexandridis, P.; Holzwarth, J. F.; Hatton, T. A. *Macromolecules* **1994**, *27*, 2414.

(6) Wanka, G.; Hoffmann, H.; Ulbricht, W. *Macromolecules* **1994**, *27*, 4145.

(7) Grant, C. D.; DeRitter, M. R.; Steege, K. E.; Fadeeva, T. A.; Castner, E. W., Jr. *Langmuir* **2005**, *21*, 1745.

(8) Linse, P.; Malmsten, M. *Macromolecules* **1992**, *25*, 5434.

(9) Malmsten, M.; Linse, P. *Macromolecules* **1992**, *25*, 5440.

(10) Zhang, K.; Khan, A. *Macromolecules* **1995**, *28*, 3807.

(11) Chu, B. *Langmuir* **1995**, *11*, 414.

(12) Alexandridis, P.; Zhou, D.; Khan, A. *Langmuir* **1996**, *12*, 2690.

(13) Lisi, R. D.; G. Lazzara, S.; Milioto, S.; Muratore, N. *J. Phys. Chem. B.* **2004**, *108*, 18214.

(14) Scherlund, M.; Welin-Berger, K.; Brodin, A.; Malmsten, M. *Eur. J. Pharm. Sci.* **2001**, *14*, 53.

(15) Rapoport, N. Y.; Herron, J. N.; Pit, W. G.; Pitina, L. *J. Controlled Release* **1999**, *58*, 153.

(16) Allen, C.; Maysinger, D.; Eisenberg, A. *Colloids Surf. B.* **1999**, *16*, 3.

(17) Varshney, M.; Morey, T. E.; Shah, D. O.; Flint, J. A.; Moudgil, B. M.; Seubert, C. N.; Dennis, D. M. *J. Am. Chem. Soc.* **2004**, *126*, 5108.

(18) Zhang, R.; Liu, J.; Han, B.; He, J.; Liu, Z.; Zhang, J. *Langmuir* **2003**, *19*, 8611.

(19) Ma, Y.; Qi, L.; Ma, J.; Cheng, H.; Shen, W. *Langmuir* **2003**, *19*, 9079.

(20) Duxin, N.; Liu, F.; Vali, H.; Eisenberg, A. *J. Am. Chem. Soc.* **2005**, *127*, 10063.

(21) Fendler, J. H. *Membrane Mimetic Chemistry*; Wiley: New York, 1982.

(22) Fukuzumi, S.; Nishimine, M.; Ohkubo, K.; Tkachenko, N. V.; Lemmetyinen, H. *J. Phys. Chem. B.* **2003**, *107*, 12511.

(23) Kumbhakar, M.; Nath, S.; Pal, H.; Sapre, A. V.; Mukherjee, T. *J. Chem. Phys.* **2003**, *119*, 388.

(24) Kumbhakar, M.; Nath, S.; Mukherjee, T.; Pal, H. *J. Chem. Phys.* **2004**, *120*, 2824.

(25) (a) Kumbhakar, M.; Nath, S.; Mukherjee, T.; Pal, H. *J. Chem. Phys.* **2005**, *122*, 084512. (b) Kumbhakar, M.; Nath, S.; Mukherjee, T.; Pal, H. *J. Chem. Phys.* **2005**, *122*, 034705.

(26) Kumbhakar, M.; Goel, T.; Mukherjee, T.; Pal, H. *J. Phys. Chem. B.* **2004**, *108*, 19246.

(27) Kumbhakar, M.; Goel, T.; Mukherjee, T.; Pal, H. *J. Phys. Chem. B.* **2005**, *109*, 14168.

(28) Nandi, N.; Bhattacharyya, K.; Bagchi, B. *Chem. Rev.* **2000**, *100*, 2013.

(29) Mortensen, K.; Brown, W. *Macromolecules* **1993**, *26*, 4128.

(30) Jain, N. J.; Aswal, V. K.; Goyal, P. S.; Bahadur, P. *J. Phys. Chem. B.* **1998**, *102*, 8452.

(31) Soni, S. S.; Sastry, N. V.; Patra, A. K.; Joshi, J. V.; Goyal, P. S. *J. Phys. Chem. B.* **2005**, *109*, 13069.

(32) Ganguly, R.; Aswal, V. K.; Hassan, P. A.; Gopalkrishnan, I. K.; Yakhmi, J. V. *J. Phys. Chem. B.* **2005**, *109*, 5653.

(33) Brown, W.; Schillén, K.; Hvidt, S. *J. Phys. Chem.* **1992**, *96*, 6038.

(34) Zhou, Z.; Chu, B. *J. Colloid Interface Sci.* **1988**, *126*, 171.

(35) Dutt, G. B. *J. Phys. Chem. B.* **2005**, *109*, 4923.

(36) Grant, C. D.; Steege, K. E.; Bunagan, M. R.; Castner, E. W., Jr. *J. Phys. Chem. B.* **2005**, *109*, 22273.

(37) Alexandridis, P.; Nivaggioli, T.; Hatton, T. A. *Langmuir* **1995**, *11*, 1468.

(38) Kabanov, A. V.; Nazarova, I. R.; Astafieva, I. V.; Batrakov, E. V.; Alakhov, V. Y.; Yaroslavov, A. A.; Kabanov, V. A. *Macromolecules* **1995**, *28*, 2303.

(39) Humpolickova, J.; Stepanek, M.; Prochazka, K.; Hof, M. *J. Phys. Chem. A.* **2005**, *109*, 10803.

(40) Sen, P.; Ghosh, S.; Sahu, K.; Mondal, S. K.; Roy, D.; Bhattacharyya, K. *J. Chem. Phys.* **2006**, *124*, 204905.

(41) Lee, J. C.-M.; Law, R. J.; Discher, D. E. *Langmuir* **2001**, *17*, 3592.

(42) Dutt, G. B. *J. Phys. Chem. B.* **2002**, *106*, 7398.

(43) Quitevis, E. L.; Marcus, A. H.; Fayer, M. D. *J. Phys. Chem.* **1993**, *97*, 5762.

(44) Maiti, N. C.; Krishna, M. M. G.; Britto, P. J.; Periasamy, N. *J. Phys. Chem. B.* **1997**, *101*, 11051.

(45) Kumbhakar, M.; Goel, T.; Mukherjee, T.; Pal, H. *J. Phys. Chem. B.* **2005**, *109*, 18528.

(46) Kumbhakar, M.; Nath, S.; Mukherjee, T.; Pal, H. *J. Chem. Phys.* **2004**, *121*, 6026.

(47) O'Connor, D. V.; Philips, D. *Time correlated single photon counting*; Academic press: New York, 1984.

(48) Maroncelli, M.; Fleming, G. R. *J. Chem. Phys.* **1987**, *86*, 6221.

(49) Edwards, J. T. *J. Chem. Educ.* **1970**, *47*, 261.

(50) Jones, G., II; Jackson, W. R.; Choi, C.; Bergmark, W. R. *J. Phys. Chem.* **1985**, *89*, 289.

(51) Palmer, P. M.; Chen, Y.; Topp, M. R. *Chem. Phys. Lett.* **2000**, *318*, 440.

(52) Chudoba, C.; Nibbering, E. T. J.; Elsaesser, T. *Phys. Rev. Lett.* **1998**, *81*, 3010.

(53) Chudoba, C.; Nibbering, E. T. J.; Elsaesser, T. *J. Phys. Chem. A.* **1999**, *103*, 5625.

(54) Nibbering, E. T. J.; Tschirschwitz, F.; Chudoba, C.; Elsaesser, T. *J. Phys. Chem. A.* **2000**, *104*, 4236.

(55) Rechthaler, K.; Köhler, G. *Chem. Phys.* **1994**, *189*, 99.

(56) Nad, S.; Pal, H. *J. Phys. Chem. A.* **2001**, *105*, 1097.

(57) Dean, J. A., Ed. *Lange's Handbook of Chemistry*, 13th ed.; McGraw-Hill: New York, 1987.

(58) Atkins, P. W. *Physical Chemistry*; Oxford University Press: Oxford, 1994.

(59) Olander, R.; Nitzan, A. *J. Chem. Phys.* **1995**, *102*, 7180.

(60) Streletzky, K.; Phillies, G. D. J. *Langmuir* **1995**, *11*, 42.

(61) Charlton, I. D.; Doherty, A. P. *J. Phys. Chem. B.* **2000**, *104*, 8327.

(62) Molina-Bolivar, J. A.; Aguiar, J.; Ruiz, C. C. *J. Phys. Chem. B.* **2002**, *106*, 870.

(63) Nandi, N.; Bagchi, B. *J. Phys. Chem. A.* **1997**, *101*, 10954.